



Research article

Development rheological and anti-corrosion property of epoxy polymer and its composite



Rachid Hsissou ^{a,c,*}, Omar Dagdag ^a, Mohamed Berradi ^b, Mehdi El Bouchti ^b, Mohammed Assouag ^c, Ahmed Elharfi ^a

^a Laboratory of Agricultural Resources, Polymers and Process Engineering, Ibn Tofail University, Faculty of Sciences, BP 133, 14000, Kenitra, Morocco

^b Laboratory REMTEX, ESITH (High School of Textile and Clothing Industries), Casablanca, Morocco

^c Team of Innovative Materials and Mechanical Manufacturing Process, ENSAM, University Moulay Ismail, B.P. 15290, Al Mansour, Meknes, Morocco

ARTICLE INFO

Keywords:

Chemical engineering
Materials chemistry
Polymer
Composite
NMR
Rheology
SEM
Corrosion

ABSTRACT

Epoxy polymer, namely, decaglycidyl pentamethylene dianiline of phosphorus (DGPMAP) was synthesized in three steps. The synthesis of epoxy polymer DGPMAP was investigated by nuclear magnetic resonance spectroscopy, rheological analysis, scanning electron microscope (SEM), stationary and transient electrochemical methods (PDP and EIS), respectively. The rheological properties of composite (DGPMAP/MDA/TiO₂) without and with different percentages of titanium dioxide (0%, 5%, 10% and 15%) increase with both the increase in frequency and with rate of load of titanium dioxide. Besides, SEM micrographs shows a good dispersion of the titanium dioxide charge in the composite (DGPMAP/MDA/TiO₂) elaborated. The results of PDP show that epoxy polymer DGPMAP acts as mixed type inhibitor and reaches maximum corrosion inhibition efficiency reaches 92 % at 10⁻³ M. Besides, EIS results indicate that DGPMAP act as good inhibitor for carbon steel in 1 M HCl solution and its efficiency reaches 91 % at 10⁻³ M of DGPMAP. Furthermore, the adsorption of DGPMAP on carbon steel surface obeyed Langmuir isotherm.

1. Introduction

Epoxy polymers are very interesting in the industrial field and are presented in an unlimited number of applications ranging from coatings to plastic in aeronautics [1, 2, 3, 4, 5, 6]. In addition, the physical and chemical properties of epoxy polymers and their composites for high potential applications are numerous: hardening, adhesive property, mechanical strength and highest resistance to corrosion [7, 8, 9, 10, 11, 12, 13, 14, 15, 16]. The carbon steel is one of the most widely employed materials for many industrial applications because of its excellent mechanical resistance. Hydrochloric acid is the most used because of its aggressive nature and its low cost. The addition of corrosion inhibitor into the aggressive solution is employed to reduce the corrosive provoked by the direct contact of acid with the metallic surface [17]. The synthesis, elaboration, formulation and identification of epoxy polymer and its composites are granted and established in the literature [18]. There are many classes of curing agents (aromatic and aliphatic amine, anhydride acid, isocyanate) which convert epoxy polymer into composite materials with a three-dimensional (3D) structure [19, 20]. The presence of

aromatic cycles give the epoxy polymer cured resistance, adhesion, thermal stability... [21, 22].

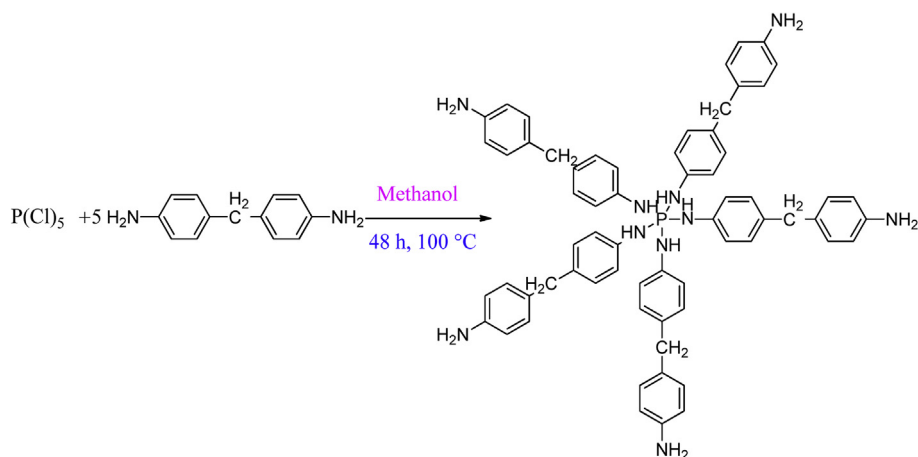
Recently, the research developed in the field of epoxy polymer aims to replace bisphenol A with a precursor without degrading the physical and chemical properties [23, 24]. In this paper, we presented the synthesis of a new epoxy polymer from a reagent containing four mobile hydrogen atoms such as methylene dianiline (MDA) with phosphorus pentachloride (PCl₅) [25].

The rheological properties of the epoxy polymer and its composite are very interesting [26]. Furthermore, the incorporation of the titanium dioxide as a load into the polymeric matrix can alter the intermolecular interaction and improve the rheological properties [27]. The improvement of the rheological properties depends on the nature of the polymer-charge interaction and dispersion quality of charge in the macromolecular matrix [28].

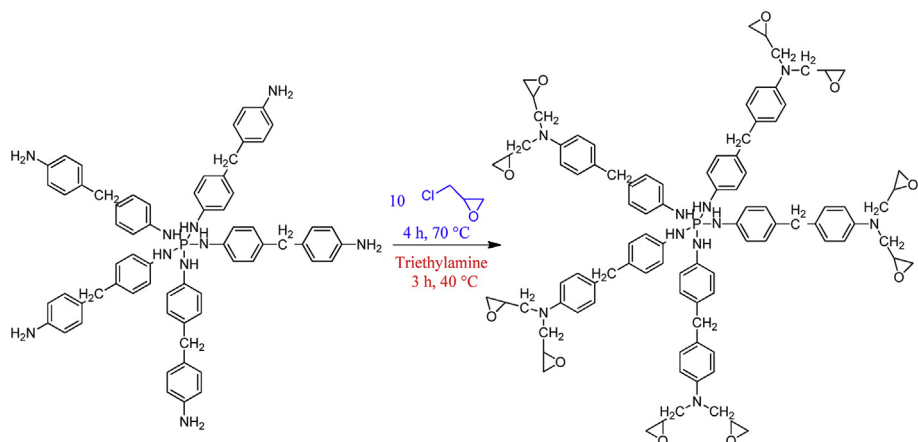
The epoxy polymer was investigated by NMR spectroscopy. Rheological properties of epoxy polymer DGPMAP and its composite (DGPMAP/MDA/TiO₂) were evaluated by the HAAK MARS rheometer. In addition, micrographs of prepared composite were determined by

* Corresponding author.

E-mail address: r.hsissou@gmail.com (R. Hsissou).



Scheme 1. Synthesis of the penta-amino pentamethylene dianiline of phosphorus.



Scheme 2. Synthesis of epoxy polymer DGPMdap.

SEM. The results of PDP and EIS show that the epoxy polymer DGPMdap is a good inhibitor for carbon steel in 1.0 M HCl solution.

2. Material and methods

2.1. Synthesis of epoxy polymer DGPMdap

The decafunctional epoxy polymer, namely, decaglycidyl of pentamethylene dianiline of phosphorus (DGPMdap) was synthesized in three steps:

In the first step, we mixed 24×10^{-3} mol of methylene dianiline with 4.8×10^{-3} mol of phosphorus pentachloride in the presence of methanol as solvent with magnetic stirring for 48 h at 100 °C (Scheme 1). During the second step, we condensed 0.048 mol of epichlorohydrin to pentamino pentamethylene dianiline of phosphorus with magnetic stirring at 70 °C for 4 h (Scheme 2). In the third step, we added 0.036 mol of the triethylamine base with magnetic stirring for 3 h at 40 °C (Scheme 2). The methanol and the triethylamine were removed by using the rotary evaporator. All the used products chemicals were purchased from Sigma Aldrich Chemical Co (world headquarters).

2.2. Hardening and formulation of epoxy polymer DGPMdap

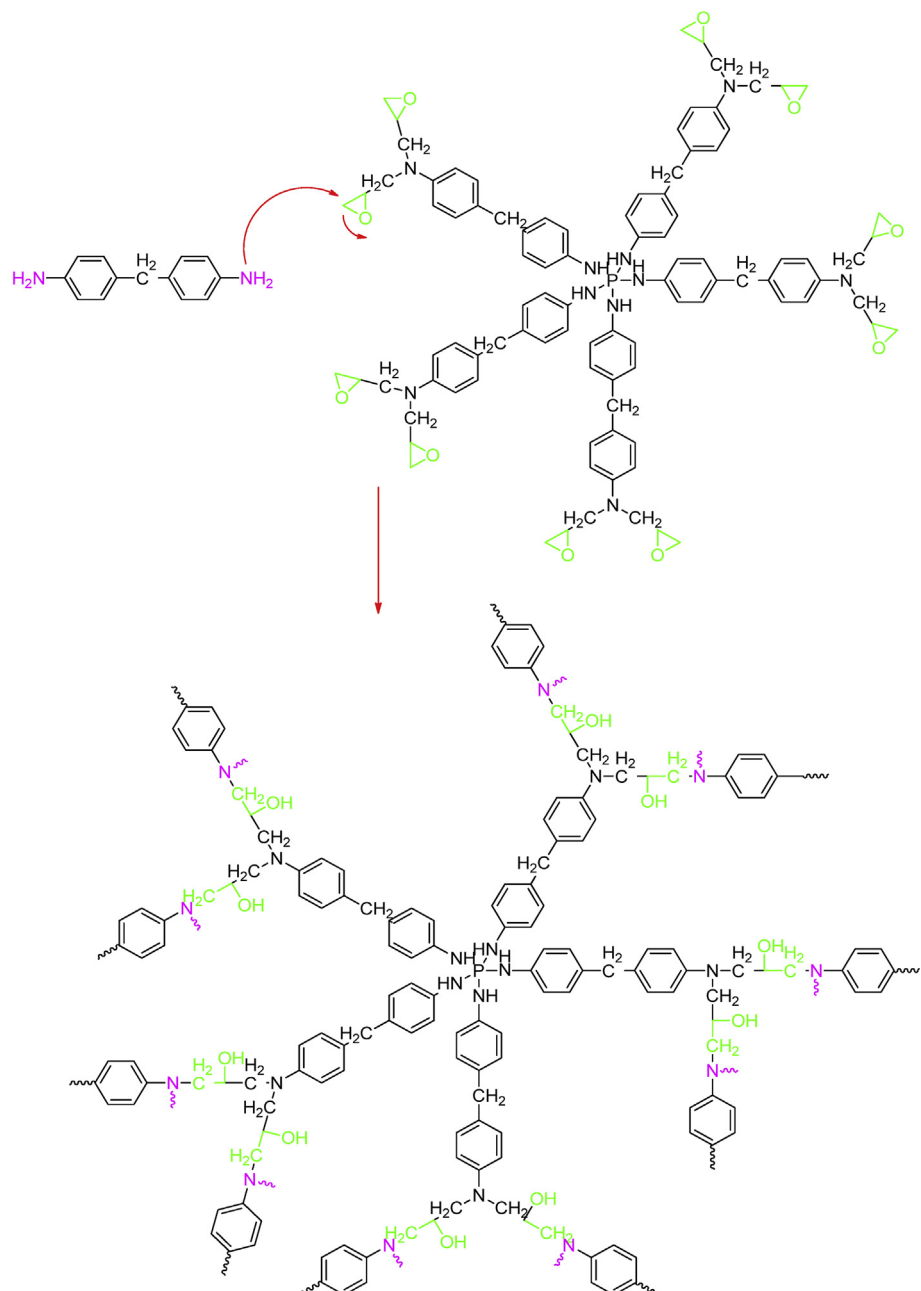
The polycondensation reaction of the decafunctional epoxy polymer DGPMdap with methylene dianiline (MDA) as hardening conducted to the formation of a three-dimensional matrix (Scheme 3). Methylenediamine bears two amine functions, of which the four hydrogens can be substituted while the formation of the three-dimensional network mainly involves condensation reactions between the oxirane rings of the polymers and the amine functions of the hardener [29]. The protocol consists of preheating the approximately stoichiometric amounts of the polymer and the hardener. Furthermore, DGPMdap and MDA are raised in oven at 70 °C and 120 °C, respectively. Then, MDA is condensed with decafunctional matrix DGPMdap to give a single liquid aspect. In addition, the prepared samples were sealed in molds in the desired geometric form for 24 h at 70 °C [5]. Besides, we performed the same protocol above in the curing reaction of 1 g of DGPMdap with 0.31 g of MDA and titanium dioxide (TiO_2) at various percentages (0%, 5%, 10% and 15%) as a filler. Finally, the final material obtained is hard, infusible and insoluble [26] (Fig. 1).

diamine bears two amine functions, of which the four hydrogens can be substituted while the formation of the three-dimensional network mainly involves condensation reactions between the oxirane rings of the polymers and the amine functions of the hardener [29]. The protocol consists of preheating the approximately stoichiometric amounts of the polymer and the hardener. Furthermore, DGPMdap and MDA are raised in oven at 70 °C and 120 °C, respectively. Then, MDA is condensed with decafunctional matrix DGPMdap to give a single liquid aspect. In addition, the prepared samples were sealed in molds in the desired geometric form for 24 h at 70 °C [5]. Besides, we performed the same protocol above in the curing reaction of 1 g of DGPMdap with 0.31 g of MDA and titanium dioxide (TiO_2) at various percentages (0%, 5%, 10% and 15%) as a filler. Finally, the final material obtained is hard, infusible and insoluble [26] (Fig. 1).

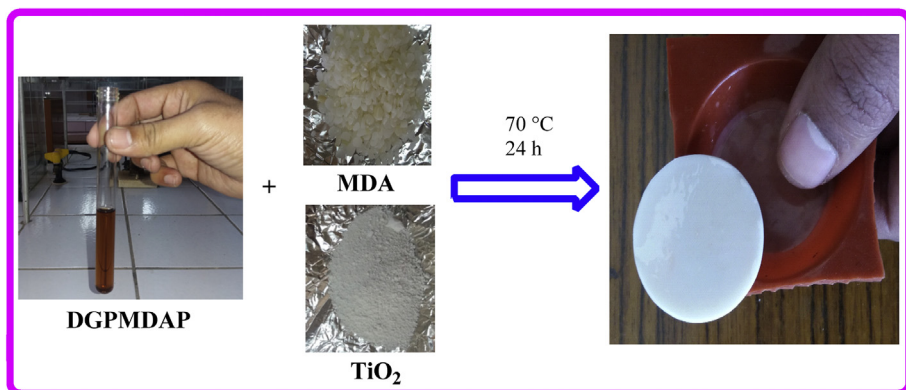
2.2.1. Ratio calculation

Decafunctional epoxy polymer DGPMdap is crosslinked with MDA in stoichiometric quantities [26]. Furthermore, epoxy equivalent weight (EEW), amine hydrogen equivalent weight (AHEW) and amount of the desired load were determined by using Eqs. (1), (2), and (3), respectively. In addition, the ratio by weight of the crosslinking relative to the decafunctional matrix was evaluated per 100 parts per hundred of epoxy resin (PHR) (Eq. 4).

$$\text{EEW} = \frac{M_w(\text{DGPMdap})}{f} \quad (1)$$



Scheme 3. Epoxy polymer DGPMAP crosslinked by MDA.

Fig. 1. Preparation of material composite (DGPMAP/MDA/TiO₂).

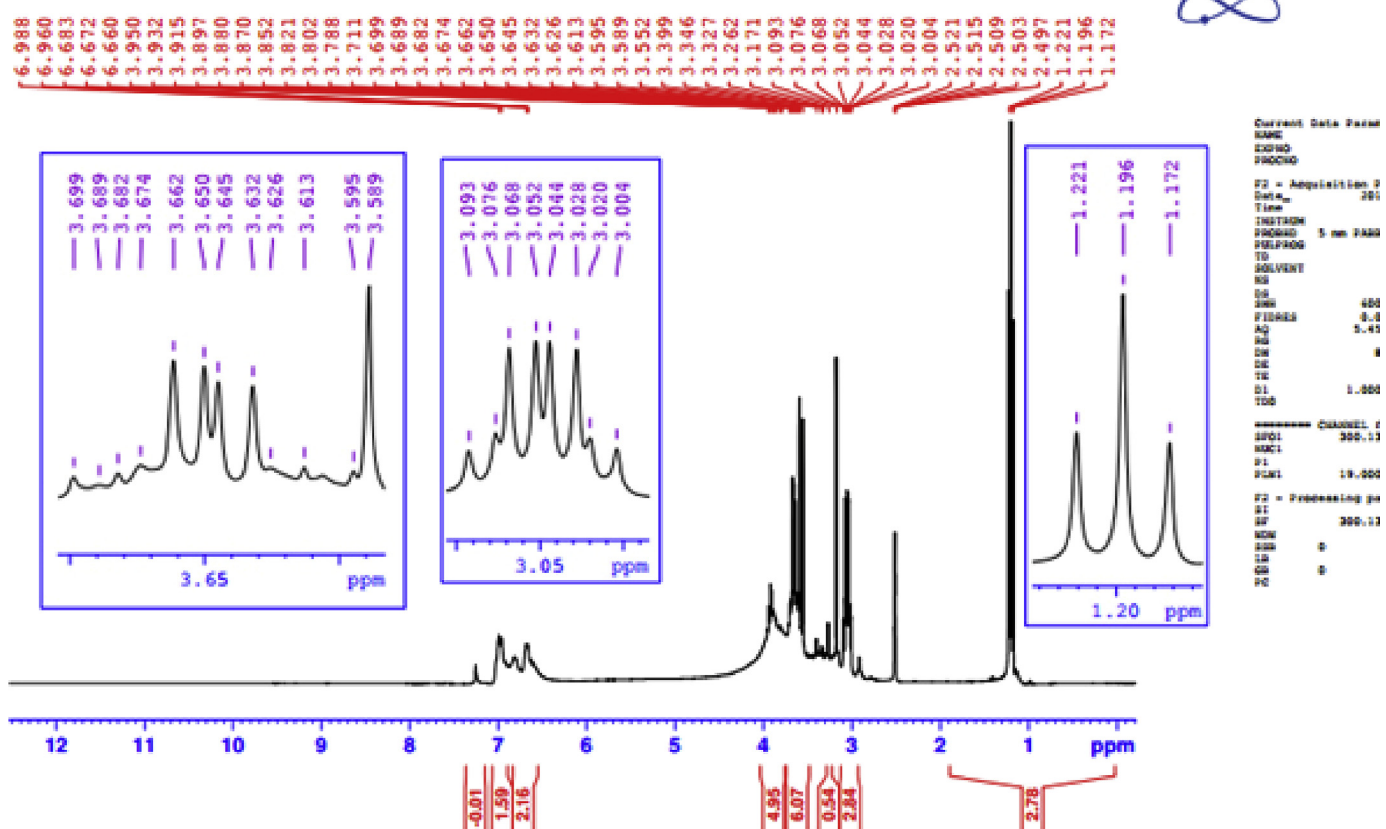


Fig. 2. ^1H NMR spectrum of DGPMMDAP.

$$AHEW = \frac{M_w(MDA)}{f} \quad (2)$$

$$y\% = \frac{x}{\text{resin} + \text{MDA} + x} \quad (3)$$

$$\text{PHR} = \frac{\text{AHEW}}{\text{EEW}} \times 100 \quad (4)$$

Where f , f' , x and y denote the number of the functionality of DGPMAP, the number of the mobile hydrogens, the amount of the DGPMAP and the amount of the titanium dioxide, respectively.

2.3. Rheological properties

Rheological properties of decafunctional epoxy polymer DGPMdap and its composite (DGPMdap/MDA/TiO₂) were evaluated according to HAAK MARS rheometer.

2.4. Stationary and transient electrochemical methods

Stationary and transient electrochemical methods were realized by means of an assembly of the electrochemical cell with three electrodes such as carbon steel (work electrode), counter electrode (platinum electrode) and reference electrode (saturated calomel), respectively. The contact surface of carbon steel with corrosive solution is 1 cm^2 . PDP study was evaluated according to potentiostat/galvanostat SP-200 Biologic Science Instruments. Carbon steel is immersed in the corrosive solution for 30 min with scanning speed of 0.5. Then, inhibition efficiency is realized according to Eq. (5). Moreover, EIS study was employed by same apparatus with a signal amplitude (10 mV). Besides, the frequency

domain used varies from 100 kHz to 10 mHz. Then, inhibition efficiency is calculated according to Eq. (6).

$$\text{IE\%} = \left(\frac{i_{corr}^0 - i_{corr}}{i_{corr}^0} \right) \times 100 \quad (5)$$

$$\text{IE\%} = \left(\frac{R_{ct} - R_{ct}^0}{R_{ct}} \right) \times 100 \quad (6)$$

With i_{corr}^0 , i_{corr} and R_{ct}^0 , R_{ct} denote the corrosion current densities and the charge transfer resistances without and in the presence of various concentrations of DGPMDA, respectively.

3. Results and discussion

3.1. Nuclear magnetic resonance

Figs. 2 and 3 show the ^1H NMR and ^{13}C NMR spectra of the deafunctional epoxy polymer DGPMAP. The alphabetical character s, d, t, q, and m denote singlet, doublet, triplet, quadruplet, and multiplet. The assignment of various chemical displacements of deafunctional epoxy polymer DGPMAP is as follows.

¹H RMN (ppm): 1.2 (solvent); 2.5 (d, 20H, CH₂ of oxirane); 3.05 (m, 10H, CH of oxirane); 3.65 (d, 20H, CH₂ bond to oxirane); 3.8 (s, 20H, CH₂ bond to benzene); 4 (s, 5H, H bond to nitrogen); 6.8–7.3 (d, 40H, aromatic hydrogen).

¹³C RMN (ppm): 41 (s, 5C, CH₂ between two benzenes); 45.8 (s, 10C, CH₂ of oxirane); 46.8 (s, 10C, CH of oxirane); 70 (s, 10C, CH₂ bond of oxirane); 112–114 (s, aromatic carbon in the ortho position of the amine II and III); 129–130 (s, aromatic carbon in the ortho position of the methylene group); 146 (s, aromatic carbon bond to amine III).

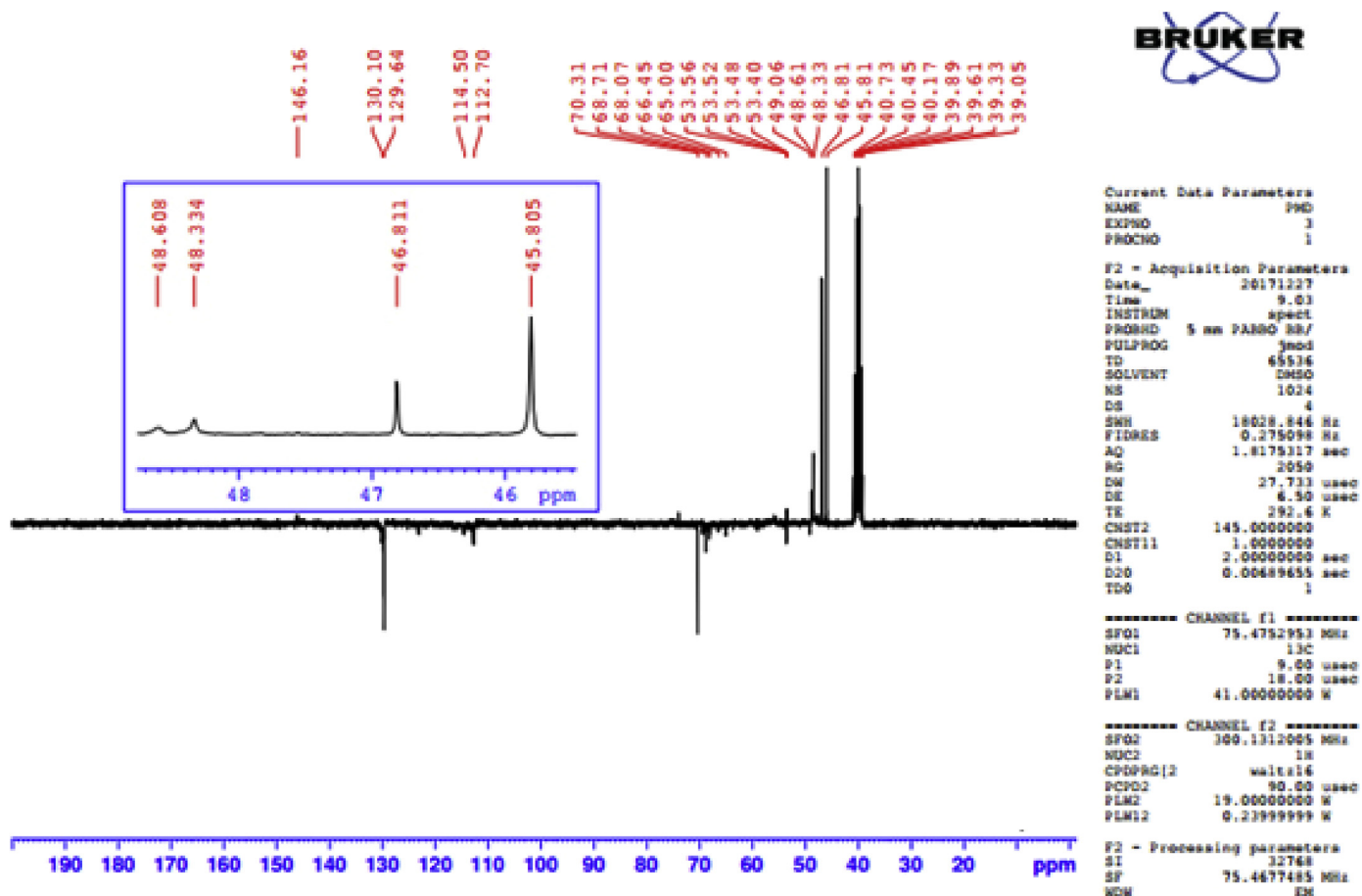


Fig. 3. ^{13}C NMR spectrum of DGPMdap.

3.2. Storage modulus (G') and loss modulus (G'')

3.2.1. G' and G'' according to temperature

Storage modulus (G') and loss modulus (G'') of decafunctional epoxy polymer DGPMdap according to temperature is presented in Fig. 4. Moreover, these rheological behaviors increase with increasing of the temperature to a glass transition temperature (T_g) [30, 31]. Then, from this T_g the G' and G'' decrease. Furthermore, at temperature below the T_g , the response of decafunctional epoxy polymer DGPMdap is of the gel type. However, at temperature above the T_g the response of

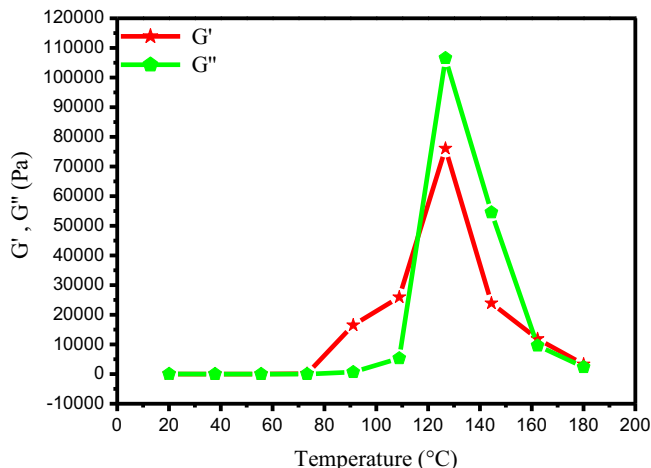


Fig. 4. G' and G'' as function of temperature.

macromolecular matrix DGPMdap is of the liquid type [32]. Additionally, the T_g of storage modulus and loss modulus are the same (127°C).

3.2.2. G' and G'' as function of frequency

Figs. 5 and 6 present G' and G'' of (DGPMdap/MDA/TiO₂) prepared composite as function of frequency at various percentage of titanium dioxide (0%, 5%, 10% and 15%) as a load, respectively [33, 34]. Furthermore, G' and G'' increase with both the increase in frequencies

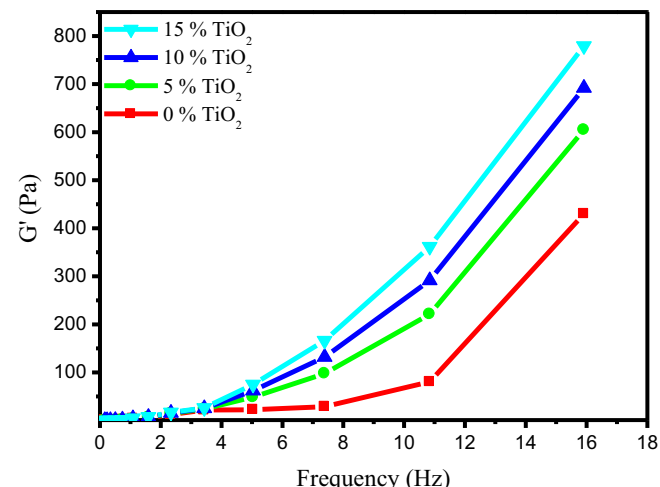


Fig. 5. G' as function of frequency at different composite (DGPMdap/MDA/TiO₂).

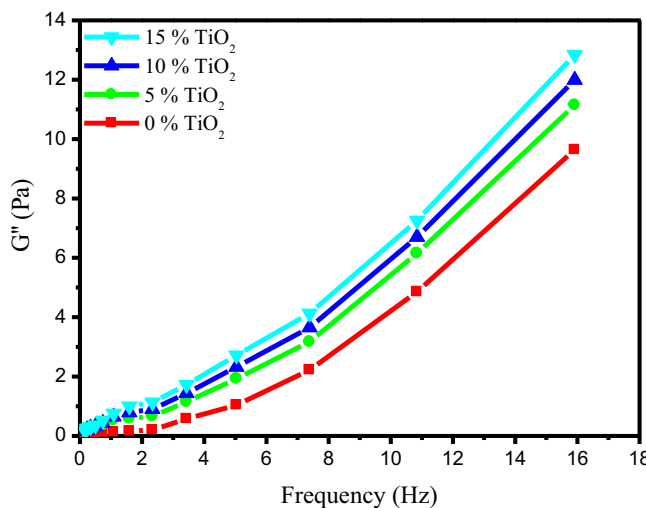


Fig. 6. G'' as function of frequency at different composite (DGPMdap/MDA/ TiO_2).

and with the rate of titanium dioxide as filler integrated in (DGPMdap/MDA/ TiO_2) composite [35]. This could explain that the charge of zinc oxide added to the various composites prepared is well formulated. Moreover, at lower frequency, the molecular relaxation process is sufficiently long, which makes the storage modulus and loss modulus measurement more sensitive. Besides, increased storage modulus and loss modulus for different composites is a common

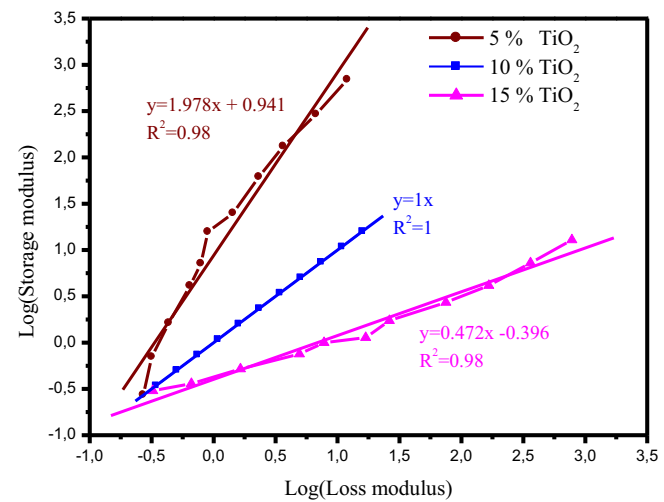


Fig. 7. Cole-Cole chart for composite (DGPMdap/MDA/ TiO_2) at different formulation.

phenomenon for epoxy prepolymer crosslinked and reinforced, which can be explained by the interaction between the DGPMdap and TiO_2 hindering the movement of the DGPMdap macromolecular chains [36, 37, 38].

Fig. 7 shows the log(G') according to log(G'') for (DGPMdap/MDA/ TiO_2) composite at different formulations. The Cole-Cole graph can be

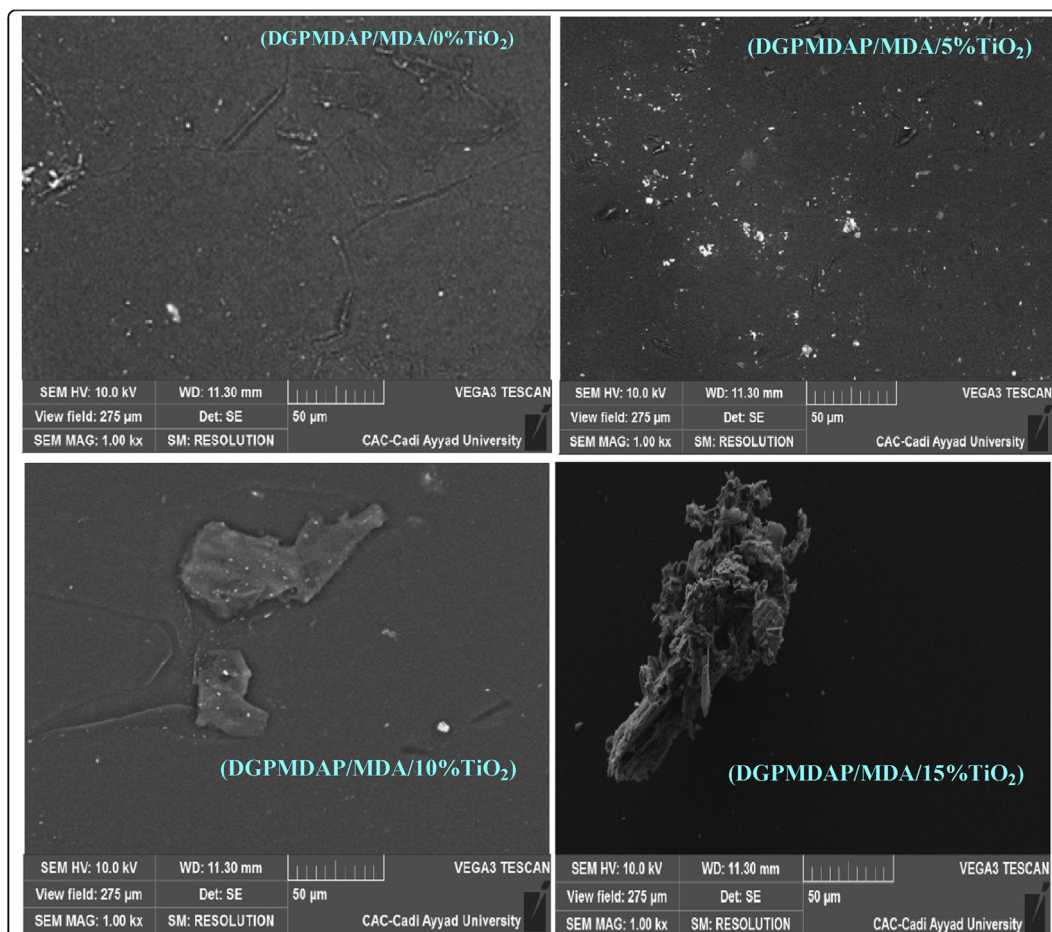


Fig. 8. Morphology of different composite (DGPMdap/MDA/ TiO_2) at various percentages (0, 5, 10 and 15%) of TiO_2 .

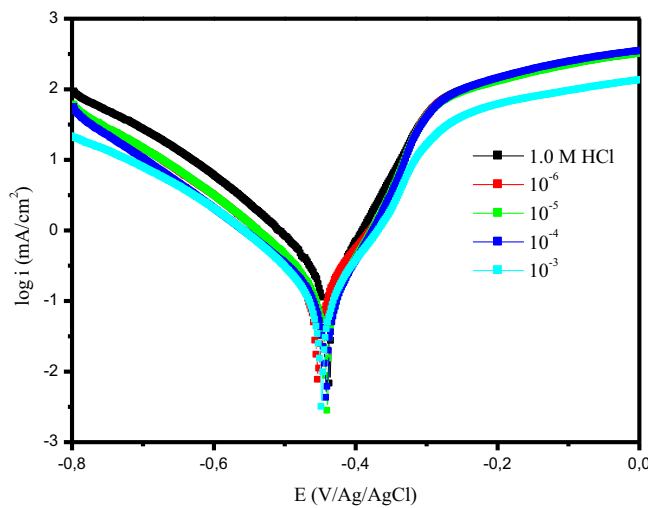


Fig. 9. PDP plot in 1 M HCl solution for carbon steel without and with various concentrations of DGPMdap.

Table 1

PDP parameters without and with various concentrations of epoxy polymer DGPMdap.

Inhibitor	Concentration (M)	$-E_{corr}$ (mV)	i_{corr} ($\mu\text{A cm}^{-2}$)	Tafel slopes (mV dec $^{-1}$)		EI (%)
				($-\beta_a$)	(β_a)	
HCl	1.0	437	259	119	68	-
DGPMdap	10^{-6}	437	72	106	56	72
	10^{-5}	439	64	63	51	75
	10^{-4}	438	28	90	48	89
	10^{-3}	447	21	24	25	92

realized to analyze the rheological behaviors of the epoxy polymer [39]. It shows a linear relationship between G' and G'' for homogeneous composites polymer. However, composite heterogeneous present the deviation occur from the line and the graph will be circle. The slope is less than 2 with a good correlation ($R^2 = 0.98, 1$ and 0.98) for the different composites. This indicated the homogeneity of the composites (DGPMdap/MDA/TiO₂) prepared. Furthermore, the composite (DGPMdap/MDA/TiO₂) with 10% of the titanium dioxide was more

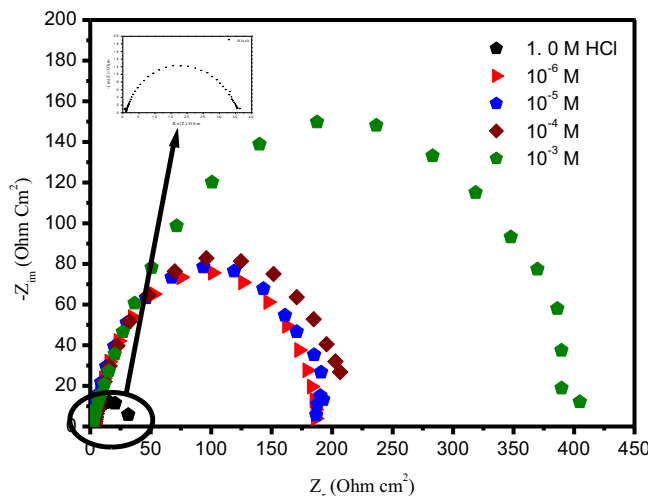


Fig. 10. Nyquist diagram in the absence and in the presence of various concentrations of DGPMdap.

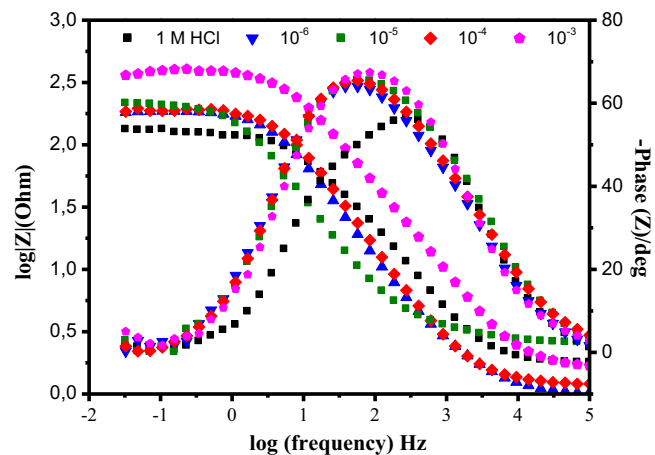


Fig. 11. Bode diagrams in the absence and in the presence of various concentrations of DGPMdap.

Table 2

EIS parameters without and in the presence of various concentrations of DGPMdap.

Inhibitor	Concentration (M)	R_s (Ωcm^2)	C_{dl} ($\mu\text{F cm}^{-2}$)	R_{ct} (Ωcm^2)	IE (%)	θ
Blank	1.0	0.456	314	38	-	
DGPMdap	10^{-6}	1.056	244.1	190	80	0.80
	10^{-5}	1.220	173.2	202	81	0.81
	10^{-4}	1.351	155.1	222	83	0.83
	10^{-3}	1.540	58.77	418	91	0.91

homogeneous than that of (5% TiO₂ and 15% TiO₂). In addition, the composite containing 15% of titanium dioxide had a viscous behavior. However, the composite containing 5% TiO₂ was more elastic [28].

3.3. Morphology of different composite (DGPMdap/MDA/TiO₂)

The SEM micrographs of (DGPMdap/MDA/TiO₂) different composites prepared without and with different percentages (0 %, 5 %, 10 % and 15 %) of TiO₂ as load were determined by using a scanning electron microscope (Fig. 8). Furthermore, the micrographs of (DGPMdap/MDA/TiO₂) different materials composites formulated at different percentages shows the good dispersion of titanium dioxide filler incorporated composite, so the quantity of the formed composite material within the charge of TiO₂ is highly formulated and the composite material chains movement is decreased [40]. This behavior indicates that homogeneous TiO₂ dispersion in the composite is solely realized at a percentage less than 15%. Some agglomerate was observable, especially at the higher particles content of TiO₂ (15%) [41].

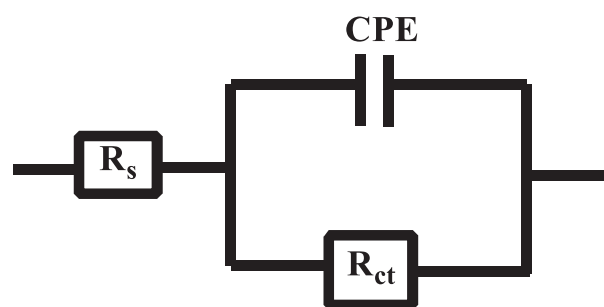


Fig. 12. ECE used.

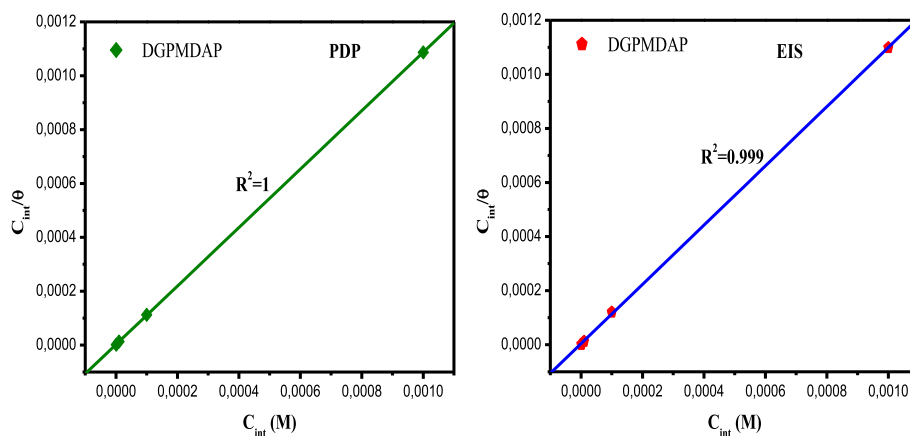


Fig. 13. Langmuir adsorption isotherm of DGPMdap by two methods (PDP and EIS) at 298 K.

Table 3
Langmuir adsorption parameters.

Inhibitor	Techniques	R ²	K _{ads} (M ⁻¹ .10 ⁶)	-ΔG° _{ads} (KJ.mol ⁻¹)
DGPMdap	PDP	1	0.46	42.72
	EIS	0.999	0.25	40.79

3.4. PDP study

PDP curves for carbon steel in corrosive solution (1 M HCl) without and with various concentrations of DGPMdap at 298 K are presented in Fig. 9. From Fig. 9, the careful observation reflects that of polarization curves without and in the presence of various concentrations are similar which indicate that epoxy polymer inhibit metallic corrosion by blocking the active sites present over the metallic surface without changing the mechanism of corrosive dissolution [42]. Obviously, this observation indicates that epoxy polymer is acted as mixed inhibitor type. Then, electrochemical parameters are grouped in Table 1. From Table 1, it is clear that i_{corr} values decreased sharply when the epoxy polymer DGPMdap was added to the corrosive environment [43, 44]. Correspondingly, the inhibitory efficiency increases with increasing of DGPMdap concentration and reaches a maximum value of 92% at 10⁻³ M. The highest inhibitory efficiency of epoxy polymer DGPMdap could be explicated due to higher molecular volume and the presence several heteroatoms that could be adsorb to metal surface. Moreover, the investigated epoxy polymer revealed relatively very good corrosion inhibitory efficiency as compared to most of the previously traditional corrosion inhibitors at lower concentration [45, 46].

3.5. EIS study

The EIS curves and Bode plots for metallic substrate in 1.0 M HCl without and with various concentrations of epoxy polymer DGPMdap at 298 K are shown in Figs. 10 and 11. The electrochemical parameters values such as resistance of solution (R_s), charge transfer resistance (R_{ct}) and double layer capability (C_{dl}) of epoxy polymer are grouped in Table 2. The results from Fig. 10 present alone capacitive loops in the Nyquist diagrams, which can be explicated to a single charge transfer resistance. From Figs. 10 and 11, careful examination of Nyquist and Bode diagrams reveals that the capacitive loop diameter increases with increasing of DGPMdap concentration [47, 48, 49]. Besides, this indicates that epoxy polymer DGPMdap was adsorbed on the metallic surface and the resistance for the corrosive dissolution of carbon steel in 1.0 M HCl solution is increasing. Furthermore, the results in Table 2 show that the double layer capability (C_{dl}) values decrease, however the charge transfer resistance values increase with the increase of DGPMdap concentration [50, 51, 52]. Then, inhibitory efficiency increases with the increase of DGPMdap and reaches 91% for 10⁻³ M of DGPMdap [53, 54, 55]. Moreover, the electrochemical equivalent circuit used to model experimental data is shown in Fig. 12. R_s, R_{ct} and CPE denote resistance of solution, charge transfer resistance and constant phase element.

3.6. Adsorption isotherm

Adsorption isotherm is employed to understand the adsorption mechanism between the atoms of inhibitor epoxy polymer as such phosphorus (P), nitrogen (N) and oxygen (O) and steel atoms at the metal surface [56]. Langmuir adsorption isotherm is calculated according to Eq. (7). Langmuir isotherm has a good straight line between C_{int} and C_{int}/θ

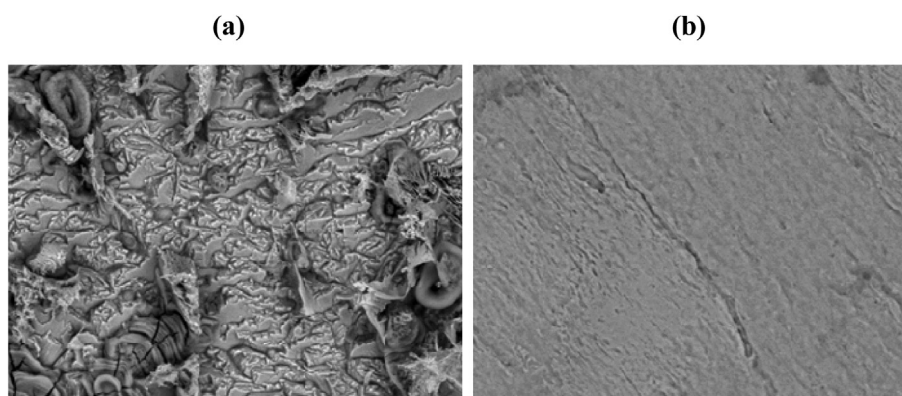


Fig. 14. Image of MEB without (a) and with (b) DGPMdap.

with intercept of K_{ads} as presented in Fig. 13. Adsorption behavior of DGPMdap on carbon steel surface obeyed with Langmuir adsorption isotherm. From the K_{ads} value, the ΔG_{ads} is determined according to Eq. (8) [57]. The highest values of K_{ads} and the lowest values of ΔG_{ads} (Table 3) indicate that epoxy polymer DGPMdap exhibits a strong interactions and a strong adsorption on the carbon steel surface (chemisorption). In addition, the linear correlation coefficient R^2 is close to 1, which result that the adsorption on the metal surface obeys the Langmuir adsorption isotherm [58].

$$\frac{C_{int}}{\theta} = \frac{1}{K_{ads}} + C_{inh} \quad (7)$$

$$K_{ads} = \frac{1}{55.5} \exp\left(\frac{-\Delta G_{ads}^\circ}{RT}\right) \quad (8)$$

With C_{inh} , θ , K_{ads} , R and T denote concentration of DGPMDA, surface coverage degree, adsorption coefficient, constant of perfect gases and the temperature.

3.7. SEM analysis

Fig. 14 represent the analysis SEM with and without the inhibitor in acidic solution after 24 h immersion. From these images, in absence of inhibitor the surface was deeply attacked by the corrosive solution with a presence of damage, including pits. In presence of 10^{-3} M of inhibitor the surface of electrode becomes smooth with disappeared of the damage and pits caused by solution corrosive that indicate, its protected effect of the molecules inhibitor on the surface of electrode [59, 60, 61].

4. Conclusion

Structure of epoxy polymer DGPMdap was investigated by using NMR spectroscopy. The results obtained from the storage modulus and loss modulus concerning the epoxy polymer DGPMdap and its composite (DGPMdap/MDA/TiO₂) formulated at different percentage of titanium dioxide load are very interesting. Besides, the micrographs of various (DGPMdap/MDA/TiO₂) composites elaborated show the very good distribution of the load. The results of PDP were consistent with results derived from EIS studies. Moreover, the adsorption of epoxy polymer DGPMdap on metal surface obeyd Langmuir adsorption isotherm. Besides, EIS revealed the adsorption of epoxy polymer are confirmed with increase in R_{ct} and decrease in C_{dl} values.

Declarations

Author contribution statement

Rachid Hsissou: Performed the experiments; Analyzed and interpreted the data, Wrote the paper.

Ahmed Elharfi: Conceived and designed the experiments.

Mohammed Assouag, Mehdi El Bouchti, Mohamed Berradi: Contributed reagents, materials, analysis tools or data.

Omar Dagdag: Analyzed and interpreted the data.

Funding statement

This research did not receive any specific grant from funding agencies in the public, commercial, or not-for-profit sectors.

Competing interest statement

The authors declare no conflict of interest.

Additional information

No additional information is available for this paper.

References

- [1] Y. Liu, A. Wilkinson, Rheological percolation behaviour and fracture properties of nanocomposites of MWCNTs and a highly crosslinked aerospace-grade epoxy resin system, Compos. Appl. Sci. Manuf. 105 (2018) 97–107.
- [2] T.V. Brantseva, S.O. Ilyin, I.Y. Gorbulova, S.V. Antonov, Y.M. Korolev, M.L. Kerber, Epoxy reinforcement with silicate particles: rheological and adhesive properties - Part II: characterization of composites with halloysite, Int. J. Adhesion Adhes. 68 (2016) 248–255.
- [3] N. Moslem, A. Reza, D. Abolfazl, Effect of cryogenic aging on nanophasified fiber metal laminates and glass/epoxy composites, Polym. Compos. 40 (2019) 2523–2533.
- [4] R.K. Raghava, L. Kwang-Pill, G.A. Iyenger, Self-assembly directed synthesis of poly (ortho-toluidine)-Metal (gold and palladium) composite nanospheres, J. Nanosci. Nanotechnol. 7 (2007) 3117–3125.
- [5] R. Hsissou, B. Benzidia, N. Hajjaji, A. Elharfi, Elaboration, electrochemical investigation and morphological study of the coating behavior of a new polymeric polyepoxide architecture: crosslinked and hybrid decaglycidyl of phosphorus pentamethylene dianiline on E24 carbon steel in 3.5% NaCl, Port. Electrochim. Acta 37 (3) (2019) 179–191.
- [6] D.R. Son, A.V. Raghu, K.R. Reddy, H.M. Jeong, Compatibility of thermally reduced graphene with polyesters, J. Macromol. Sci. Part B: Phys. 55 (2016) 1099–1110.
- [7] M.U. Khan, K.R. Reddy, T. Snguanwongchai, E. Haque, V.G. Gomes, Polymer brush synthesis on surface modified carbon nanotubes via in situ emulsion polymerization, Colloid Polym. Sci. 294 (2016) 1599–1610.
- [8] R. Hsissou, A. Elharfi, Application of pentaglycidyl ether penta-ethoxy phosphorus composites polymers formulated by two additives, Trisodium Phosphate (TSP) and Natural phosphate (NP) and their combination in the behavior of the coating on E24 carbon steel in NaCl 3.5%, Anal. Bioanal. Electrochem. 10 (6) (2018) 728–738.
- [9] K.R. Reddy, B.C. Sin, K.S. Ryu, J.C. Kim, H. Chung, Y. Lee, Conducting polymer functionalized multi-walled carbon nanotubes with noble metal nanoparticles: synthesis, morphological characteristics and electrical properties, Synth. Met. 159 (2009) 595–603.
- [10] Y.P. Zhang, S.H. Lee, K.R. Reddy, A.I. Gopalan, K.P. Lee, Synthesis and characterization of core-shell SiO₂ nanoparticles/poly(3-aminophenylboronic acid) composites, J. Appl. Polym. Sci. 104 (2007) 2743–2750.
- [11] K.R. Reddy, K.P. Lee, A.I. Gopalan, Novel electrically conductive and ferromagnetic composites of poly(aniline-co-aminonaphthalenesulfonic acid) with iron oxide nanoparticles: synthesis and characterization, J. Appl. Polym. Sci. 106 (2007) 1181–1191.
- [12] M. Hassan, K.R. Reddy, E. Haque, S.N. Faisal, S. Ghasemi, A.I. Minett, V.G. Gomes, Hierarchical assembly of graphene/polyaniline nanostructures to synthesize free-standing supercapacitor electrode, Compos. Sci. Technol. 98 (2014) 1–8.
- [13] K.R. Reddy, K.P. Lee, Y. Lee, A.I. Gopalan, Facile synthesis of conducting polymer–metal hybrid nanocomposite by in situ chemical oxidative polymerization with negatively charged metal nanoparticles, Mater. Lett. 62 (2008) 1815–1818.
- [14] Y.R. Lee, S.C. Kim, H. Lee, H.M. Jeong, A.V. Raghu, K.R. Reddy, B.K. Kim, Graphite oxides as effective fire retardants of epoxy resin, Macromol. Res. 19 (2011) 66–71.
- [15] K.R. Reddy, K.P. Lee, A.I. Gopalan, Self-assembly approach for the synthesis of electro-magnetic functionalized Fe3O4/polyaniline nanocomposites: effect of dopant on the properties, Colloids Surf., A 320 (2008) 49–56.
- [16] K.R. Reddy, H.M. Jeong, Y. Lee, A.V. Raghu, Synthesis of MWCNTs-core/thiophene polymer-sheath composite nanocables by a cationic surfactant-assisted chemical oxidative polymerization and their structural properties, J. Polym. Sci., Polym. Chem. Ed. Part A 48 (2010) 1477–1484.
- [17] R. Hsissou, B. Benzidia, M. Rehioui, M. Berradi, A. Berisha, M. Assouag, N. Hajjaji, A. Elharfi, Anticorrosive property of hexafunctional epoxy polymer HGTMADAE for E24 carbon steel corrosion in 1.0 M HCl: gravimetric, electrochemical, surface morphology and molecular dynamic simulations, Polym. Bull. (2019).
- [18] A.M. Atta, R. Mansour, M.I. Abdou, A.M. El-Sayed, Synthesis and characterization of tetra-functional epoxy resins from rosin, J. Polym. Res. 12 (2) (2005) 127–138.
- [19] E.O. Ozgul, M.H. Ozkul, Effects of epoxy, hardener, and diluent types on the workability of epoxy mixtures, Constr. Build. Mater. 158 (2018) 369–377.
- [20] R. Hsissou, B. Benzidia, N. Hajjaji, A. Elharfi, Elaboration and electrochemical studies of the coating behavior of a new pentafunctional epoxy polymer: pentaglycidyl ether pentabiphenol A phosphorus on E24 carbon Steel in 3.5% NaCl, Journal of Chemical Technology and Metallurgy 53 (2018) 898–905.
- [21] S. Flint, T. Markle, S. Thompson, E. Wallace, Bisphenol A exposure, effects, and policy: a wildlife perspective, J. Environ. Manag. 104 (2012) 19–34.
- [22] R. Hsissou, A. Bekhta, A. Elharfi, Synthesis and characterization of a new epoxy resin homologous of DGEBA diglycidyl bis disulfide carbon ether of bisphenol A, J. Chem. Technol. Metall. 53 (3) (2018) 414–421.
- [23] P. Niedermann, G. Szekely, A. Toldy, Novel high glass temperature sugar-based epoxy resins: characterization and comparison to mineral oil-based aliphatic and aromatic resins, Express Polym. Lett. 9 (2) (2015) 85–94.
- [24] O. Dagdag, Z. Safi, R. Hsissou, H. Erramli, M. El Bouchti, N. Wazzan, L. Guo, C. Verma, E.E. Ebenso, A. Elharfi, Epoxy pre-polymers as new and effective materials for corrosion inhibition of carbon steel in acidic medium: computational and experimental studies, Sci. Rep. 9 (2019) 11715.

- [25] R. Hsissou, M. Berradi, M. El Bouchti, A. El Bachiri, A. Elharfi, Synthesis characterization rheological and morphological study of a new epoxy resin pentaglycidyl ether pentaphenoxy of phosphorus and their composite (PGEPPP/MDA/PN), *Polym. Bull.* 76 (9) (2019) 4859–4878.
- [26] R. Hsissou, A. Elharfi, Rheological behavior of three polymers and their hybrid composites (TGEEBA/MDA/PN), (HGEMDA/MDA/PN) and (NGHPBAE/MDA/PN), *J. King Saud Univ. Sci.* (2018).
- [27] L. Elias, F. Fenouillet, J.C. Majesté, P. Alcoufe, P. Cassagnau, Immiscible polymer blends stabilized with nano-silica particles: rheology and effective interfacial tension, *Polymer* 49 (20) (2018) 4378–4385.
- [28] S. Banafsheh, Y. Mostafa, R. Behzad, Rheological behavior of polypropylene/carbon quantum dot nanocomposites: the effects of particles size, particles/matrix interface adhesion, and particles loading, *Polym. Bull.* 76 (2018) 4335–4354.
- [29] R. Hsissou, H. Benassaoui, F. Benhiba, N. Hajjaji, A. Elharfi, Application of a new trifunctional epoxy prepolymer: triglycidyl Ether Ethenyl Bisphenol A (TGEEBA) in the coating of E24 steel in NaCl 3.5%, *J. Chem. Technol. Metall.* 52 (3) (2017) 431–438.
- [30] A.Y. Zubarev, S. Odenbach, Rheological properties of dense ferrofluids. Effet of chain-like aggregates, *J. Magn. Magn. Mater.* 252 (2002) 241–243.
- [31] M. Cvek, M. Mrlik, V. Pavlinek, A rheological evaluation of steady shear magnetorheological flow behavior using three-parameter viscoplastic models, *J. Rheol.* 60 (2016) 687–694.
- [32] O. Pozo, D. Collin, H. Finkelmann, D. Roger, P. Martonoty, Gel-like elasticity in glass-forming side-chain liquid-crystal polymers, *Phys. Rev. E* 80 (2009), 031801.
- [33] A. Momeni, M. Joseph Filiaggi, Rheology of polyphosphate coacervates, *J. Rheol.* 60 (2016) 25–34.
- [34] A. Abdenadher, M. Vincent M, T. Budtova, Rheological properties of molten flax- and Tencel®-polypropylene composites: influence of fiber morphology and concentration, *J. Rheol.* 60 (2016) 191–202.
- [35] X. Wang, S. Heng, L. Weiyang, D. Miao, Y. Song, Complex rheological behaviors of loach (*Misgurnus anguillicaudatus*) skin mucus, *J. Rheol.* 59 (2015) 51–63.
- [36] R. Hsissou, A. Bekhta, A. Elharfi, Viscosimetric and rheological studies of a new trifunctional epoxy pre-polymer with novolan ethylene: triglycidyl Ether of Ethylene of Bisphenol A (TGEEBA), *J. Mater. Environ. Sci.* 8 (2) (2017) 603–610.
- [37] Y. Song, Q. Zheng, Linear rheology of nanofilled polymers, *J. Rheol.* 59 (2015) 155–192.
- [38] R. Hsissou, M. El Bouchti, A. Elharfi, Elaboration and viscosimetric, viscoelastic and rheological studies of a new hexafunctional polyepoxide polymer: hexaglycidyl Ethylene of Methylene Dianiline, *J. Mater. Environ. Sci.* 8 (12) (2017) 4349–4361.
- [39] J.F. Zhang, X.S. Yi, Dynamic rheological behavior of high-density polyethylene filled with carbon black, *J. Appl. Polym. Sci.* 86 (14) (2002) 3527–3531.
- [40] T. Kuilla, S. Bhadra, D. Yao, N.H. Kim, S. Bose, J. Hee Lee, Recent advances in graphene based polymer composites, *Prog. Polym. Sci.* 35 (2010) 1350–1375.
- [41] J.C. Mendes, R.R. Barreto, A.C. Barbieri Paula, F.P. Eloí, G.J. Brigolini, R.A.F. Peixoto, On the relationship between morphology and thermal conductivity of cement-based composites, *Journal of Cement and Concrete Composites* 104 (2019) 103365.
- [42] R. Hsissou, S. Abbout, A. Berisha, M. Berradi, M. Assouag, N. Hajjaji, A. Elharfi, Experimental, DFT and molecular dynamics simulation on the inhibition performance of the DGDCBA epoxy polymer against the corrosion of the E24 carbon steel in 1.0M HCl solution, *J. Mol. Struct.* 1182 (2019) 340–351.
- [43] L. Weihua, H. Lichao, Z. Shengtao, H. Baorong, Effects of two fungicides on the corrosion resistance of copper in 3.5% NaCl solution under various conditions, *Corros. Sci.* 53 (2011) 735–745.
- [44] A. Anagri, A. Baitukha, C. Debiemme-Chouvy, I.T. Lucas, J. Pulpytel, T.T. Mai Tran, S. Tabibian, F.A. Khonsari, Nanocomposite coatings based on graphene and siloxane polymers deposited by atmospheric pressure plasma. Application to corrosion protection of steel, *Surf. Coat. Technol.* 377 (2019) 124928.
- [45] M.A. Amin, K.F. Khaled, Copper corrosion inhibition in O₂-saturated H₂SO₄ solutions, *Corros. Sci.* 52 (2010) 1194–1204.
- [46] H. Kaur, J. Sharma, D. Jindal, R.K. Arya, S.K. Ahuja, S.B. Arya, Crosslinked polymer doped binary coatings for corrosion protection, *Prog. Org. Coat.* 125 (2018) 32–39.
- [47] R. Hsissou, O. Dagdag, S. About, F. Benhiba, M. Berradi, M. El Bouchti, A. Berisha, N. Hajjaji, A. Elharfi, Novel derivative epoxy resin TGETET as a corrosion of E24 carbon steel in 1.0 M HCl solution. Experimental and computational (DFT and MD simulations) methods, *J. Mol. Liq.* 284 (2019) 182–192.
- [48] N.H. Othman, M.C. Ismail, M. Mustapha, N. Sallih, K.E. Kee, R.A. Jaal, Graphene-based polymer nanocomposites as barrier coatings for corrosion protection, *Prog. Org. Coat.* 135 (2019) 82–99.
- [49] R. Hsissou, A. Bekhta, A. Elharfi, B. Benzidja, N. Hajjaji, Theoretical and electrochemical studies of the coating behavior of a new epoxy polymer: hexaglycidyl Ethylene of Methylene Dianiline (HGEMDA) on E24 steel in 3.5% NaCl, *Port. Electrochim. Acta* 36 (2) (2018) 101–117.
- [50] C. Verma, M.A. Quraishi, A. Singh, 2-Amino-5-nitro-4,6-diarylhex-1-ene-1,3,3-tricarbonitriles as new and effective corrosion inhibitors for mild steel in 1 M HCl: experimental and theoretical studies, *J. Mol. Liq.* 212 (2015) 804–812.
- [51] M. Yadav, L. Gope, N. Kumari, P. Yadav, Corrosion inhibition performance of pyranopyrazole derivatives for mild steel in HCl solution: gravimetric, electrochemical and DFT studies, *J. Mol. Liq.* 216 (2016) 78–86.
- [52] X. Zhu, Y. Wu, W. Zhao, J. Pu, D. Yang, Q. Xue, Large-area preparation of defect-repaired fluorocarbon polymer coatings on graphene for long-term corrosion resistance, *Prog. Org. Coat.* 134 (2019) 234–243.
- [53] C. Verma, E.E. Ebano, I. Bahadur, 5-(Phenylthio)-3H-pyrrole-4-carbonitriles as effective corrosion inhibitors for mild steel in 1 M HCl: experimental and theoretical investigation, *J. Mol. Liq.* 212 (2015) 209–218.
- [54] Rachid Hsissou, Bouchra Benzidja, Najat Hajjaji, Elharfi Ahmed, Elaboration and electrochemical studies of the coating behavior of a new nanofunctional epoxy polymer on E24 steel in 3.5% NaCl, *Port. Electrochim. Acta* 36 (4) (2018) 259–270.
- [55] F. Ubaid, A.B. Radwan, N. Naeem, R.A. Shakoor, Z. Ahmad, M.F. Montemor, R. Kahraman, A.M. Abdullah, A. Soliman, Multifunctional self-healing polymeric nanocomposite coatings for corrosion inhibition of steel, *Surf. Coat. Technol.* 372 (2019) 121–133.
- [56] H.M.A. El-Lateef, K.A. Soliman, A.H. Tantawy, Novel synthesized Schiff Base-based cationic gemini surfactants: electrochemical investigation, theoretical modeling and applicability as biodegradable inhibitors for mild steel against acidic corrosion, *J. Mol. Liq.* 232 (2017) 478–498.
- [57] I.B. Obot, S.A. Umoren, Z.M. Gasem, R. Suleiman, B. El Ali, Theoretical prediction and electrochemical evaluation of vinylimidazole and allylimidazole as corrosion inhibitors for mild steel in 1 M HCl, *J. Ind. Eng. Chem.* 21 (2015) 1328–1339.
- [58] D. A Lopez, S.N. Simison, S.R. Sanchez, The influence of steel microstructure on CO₂ corrosion. EIS studies on the inhibition efficiency of benzimidazole, *Electrochim. Acta* 48 (2003) 845–854.
- [59] H. Pulikkalparambil, S. Siengchin, J. Parameswaranpillai, Corrosion protective self-healing epoxy resin coatings based on inhibitor and polymeric healing agents encapsulated in organic and inorganic micro and nanocontainers, *Nano-Struct. Nano-Objects* 16 (2018) 381–395.
- [60] O. Dagdag, R. Hsissou, A. Berisha, H. Erramli, O. Hamed, S. Jodeh, A. Elharfi, Polymeric based epoxy cured with a polyaminoamide as an anticorrosive coating for aluminum 2014-T3 surface: experimental studies supported by computational modeling, *J. Bio-and Triboro-Corros.* 5 (2019) 58.
- [61] M. Yang, J. Wu, D. Fang, B. Li, Y. Yang, Corrosion protection of waterborne epoxy coatings containing mussel-inspired adhesive polymers based on polyaspartamide derivatives on carbon steel, *J. Mater. Sci. Technol.* 34 (2018) 2464–2471.